HYBRID-TREFFTZ FINITE ELEMENT FORMULATION FOR SPECTRAL ELASTODYNAMIC ANALYSIS

C. Cismasiu[1] *and J.A.T. Freitast*[2]
Instituto Superior Técnico, Departamento de Engenharia Civil
1096 Lisboa CODEX, Portugal

SUMMARY

The displacement model of the hybrid-Trefftz finite element formulation is applied to the spectral elastodynamic analysis of bounded and unbounded media. Two alternative elements to model unbounded media are developed and tested, namely a bounded finite element with absorbing boundary conditions and an unbounded element that satisfies the Sommerfeld condition. Numerical tests are presented to illustrate the performance of the finite element formulation.

Keywords: Hybrid finite elements, displacement elements, Trefftz method, spectral elastodynamics, unbounded media.

1. INTRODUCTION

The theoretical basis for the development of the displacement and stress variants of the hybrid-Trefftz finite element formulation for elastodynamic analysis in the frequency domain is presented in [4].

The objective of this paper is to report on the numerical implementation of the displacement model of the hybrid-Trefftz formulation in the analysis of both bounded and unbounded media [6]. The element is hybrid because two fields are independently approximated in the domain and on the boundary of the element. The Trefftz label identifies the special feature of constraining the domain approximation basis to satisfy locally the governing wave equation. Finally, the element is said to be a displacement element because the displacement field is the one selected for direct approximation in the domain of the element. Consistently with this design, the tractions or Cauchy stresses is the boundary field, which is also approximated. The corresponding approximation basis is used to enforce the inter-element and boundary displacement continuity conditions, using a Galerkin technique. A comprehensive set of numerical tests, addressing the analysis of both bounded and unbounded media are used to show the performance of the present formulation. In the latter case, the solutions obtained with bounded finite elements with absorbing boundary conditions and with unbounded elements that implicitly satisfy the Sommerfeld condition are directly compared and assessed. Solutions

[1] PhD student
[2] Professor of Structural Engineering

obtained with the hybrid-Trefftz displacement elements are also compared with alternative formulations.

2. FUNDAMENTAL RELATIONS

Let V represent the domain of the element and Γ the enveloping surface, referred to a Cartesian system x. The fundamental frequency domain relations governing the linear elastodynamic response of the structure to a non-trivial forcing frequency w are the following:

$$Ds + w^2 r\, u = 0 \text{ in } V \qquad (1)$$

$$e = D^* u \text{ in } V \qquad (2)$$

$$s = ke \text{ in } V \qquad (3)$$

$$Ns = t_\Gamma \text{ on } \Gamma_s \qquad (4)$$

$$u = u_\Gamma \text{ on } \Gamma_u \qquad (5)$$

$$Ns = cu \text{ on } \Gamma_a \qquad (6)$$

For simplicity of the presentation, the effects of the body forces and of residual stresses are neglected. The simulation of these effects as well as the representation of the forced and free vibration modes and of the elastostatic response of the structure are contemplated in [4] and [5].

In the dynamic equilibrium (1) and compatibility (2) equations, vectors s and e collect the independent components of the stress and strain tensors and u is the displacement vector. As a geometrically linear model is assumed, the differential equilibrium and compatibility operators D and D^* are linear and adjoint.

In the equilibrium (1) and the elasticity (3) conditions, the generalized mass r and stiffness k matrices may not be Hermitian as they combine the mass r_o and the structural d_o and the elastic k_o and the material c_o damping effects, respectively:

$$r = r_o - iw^{-1} d_o \qquad k = k_o + iw\, c_o$$

In the Neumann condition (4), vector t_Γ defines the tractions prescribed on portion Γ_s of the boundary and the boundary equilibrium matrix N collects the components of the unit outward normal vector associated with the differential operators present in D. In the Dirichlet condition (5), vector u_Γ defines the displacements prescribed on the complementary portion of the boundary, Γ_u. In the Sommerfeld condition (6) for unbounded media, c is the non-Hermitian damping matrix [7].

The equations summarized above are constrained to geometrically and physically linear problems. However, they hold for inhomogeneous and multi-phase media and for alternative structural models, as the variables, arrays and operators are identified above in the generalized sense.

3. SPACE DISCRETIZATION

Let V^e denote the domain of a typical finite element and Γ^e to be the enveloping surface. No particular constraints are placed on the geometry of the element, which may not be convex, simply connected or bounded. However, as it is illustrated in Fig. l, the

identification of the Dirichlet boundary Γ_u is extended to include the set of internal, inter-element boundaries of the element when inserted in the finite element mesh. Moreover, the Sommerfeld boundary Γ_a is non-empty only for the bounding elements subject to the absorbing condition (6).

The approximations from which the hybrid-Trefftz displacement element is derived from are the following, where subscripts *V*, *u* and *a* are used to identify arrays defined in the domain V^e and on boundaries Γ_u and Γ_a, respectively:

$$u = U_V q_V \text{ in } V^e \tag{7}$$

$$t = T_u p_u \text{ on } \Gamma_u^e \tag{8}$$

$$t = T_a p_a \text{ on } \Gamma_a^e \tag{9}$$

In the definitions above, matrices U_V and T_u and T_a collect displacement and traction approximation functions. As they are selected from hierarchical (non-nodal) bases, the weighing vectors q_V, and p_u and p_a represent generalized displacements and tractions. respectively.

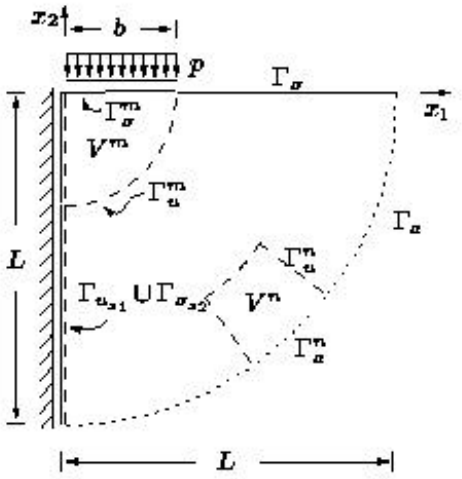

Fig. 1: Identification of the Neumann, Dirichlet and Sommerfedd boundaries.

The Trefftz constraint consists in assuming that the displacement approximation basis is built on solutions of the governing wave equation, derived combining the equilibrium, compatibility and elasticity equations (1) to (3):

$$(DkD^* + \omega^2 \rho) U_V = O \qquad \text{in } V^e \tag{10}$$

Consequently the displacement approximation (7) is uniquely associated with the strain and stress fields (11) and (12), where $E_V = D^* U_V$ and $S_V = k E_V$:

$$e = E_V q_V \text{ in } V^e \tag{11}$$

$$s = S_V q_V \text{ in } V^e \tag{12}$$

It is important to note that the definitions above are not used as direct approximations in the derivation of the hybrid-Trefftz displacement element. They are used in the post-processing phase to compute the stress and strain fields in the element, while condition (10) is exploited to obtain boundary integral expressions for matrices and vectors present in the governing system.

4. FINITE ELEMENT EQUATIONS

Using the procedure presented in [4], extended now to include the Sommerfeld absorbing boundary condition (6) and the approximation (9) for the associated tractions, the following finite element governing system is found:

$$\begin{bmatrix} D_\Gamma & -B_a & B_u \\ -B_a^T & D_a & O \\ -B_u^T & O & O \end{bmatrix} \begin{Bmatrix} q_v \\ p_a \\ p_u \end{Bmatrix} = \begin{Bmatrix} p_\Gamma \\ 0 \\ q_\Gamma \end{Bmatrix} \tag{13}$$

The finite element arrays appearing in the system (13) are defined as follows:

$$D_\Gamma = \int U_V^T N S_V \, \mathrm{d}\Gamma^e \tag{14}$$

$$B_u = \int U_V^T T_u \, \mathrm{d}\Gamma_u^e \tag{15}$$

$$B_a = \int U_V^T T_a \, \mathrm{d}\Gamma_a^e \tag{16}$$

$$D_a = \int T_a^T c^{-1} T_a \, \mathrm{d}\Gamma_a^e \tag{17}$$

$$p_\Gamma = \int U_V^T t_\Gamma \, \mathrm{d}\Gamma_s^e \tag{18}$$

$$q_\Gamma = \int T_u^T u_\Gamma \, \mathrm{d}\Gamma_u^e \tag{19}$$

In all the above equations, A^T denotes the (conjugate) transpose of a real (complex) array A. System (13) is Hermitian only when the same property applies to the local stiffness and mass matrices k and c and when no Sommerfeld boundary or unbounded element exists.

To assemble the system for a given finite element mesh, it suffices to assign symmetric boundary traction distribution (8) to the corresponding sides of connected elements. Vector p_Γ is determined directly from definition (18), applied to the Neumann boundary of the assembled mesh. The entries of vector q_Γ are set to zero on inter-element boundaries (average inter-element displacement continuity condition) and computed from definition (19) on the Dirichlet boundary of the assembled mesh.

The assembled system is highly sparse and strongly localized, in the sense that the generalized displacements q_V and the tractions p_a are strictly element dependent and the generalized boundary tractions p_u are shared only by pairs of connecting elements. This property renders the hybrid-Trefftz displacement element particularly well suited to parallel processing. The procedures used in the storing and solving these systems are adapted to exploit their high sparsity.

5. APPROXIMATION BASES FOR BOUNDED ELEMENTS

The displacement approximation basis U_V is derived from the gradient and rotational terms of the scalar potentials Φ_1 and Φ_2, respectively, which, when inserted in the wave equation (10), are found to identify with the solution spaces of the Helmholtz equation (20), where c_1 and c_2 represent the propagation velocities of the P- and S-waves, respectively:

$$\nabla^2 \Phi_k + \left(\frac{w}{c_k} \right)^2 \Phi_k = 0 \tag{20}$$

Both Cartesian (x_1,x_2) and polar (r,q) coordinate systems were used to model the homogeneous and isotropic two-dimensional applications, which are associated with displacement potentials based on exponential and Bessel functions, respectively. The traction approximation basis on the Dirichlet and Sommerfeld boundaries is built on Chebyshev polynomials, defined on the side coordinate system.

6. APPROXIMATION BASES FOR UNBOUNDED ELEMENTS

As the Sommerfeld radiation condition is supposed to hold infinity [2], a clear limitation in using the bounded elements with absorbing boundary is that Γ_a should be placed far from the excitation source when modelling an infinite media.

The fact that the stress and displacement fields generated by the Helmholtz potential, when a Hankel basis is used, satisfy locally the Sommerfeld condition for large asymptotic approximations, suggests the extension of the hybrid-Trefftz displacement formulation to unbounded elements. Hankel functions and Fourier approximations are now used to build the traction approximation basis on the unbounded and bounded Dirichlet domains, respectively. The particular geometry of the unbounded element can be exploited to obtain closed form expressions for the arrays present in the governing system. The formulae on indefinite integrals of products of Bessel functions collected in [1] have been used to derive such formulae. However, the authors could not establish such solutions for the integrals involving the direct interaction of P- and S-waves. The corresponding coefficients are computed numerically, which poses particular difficulties in terms of convergence due to the highly oscillatory nature of the integrand function. This difficulty is not experienced in the integration of the bounded element matrices and represents the price paid to avoid dimensioning *a priori* the finite element mesh to locate conveniently the absorbing boundary.

7. NUMERICAL TESTS

7.1. Comparison of the F.E. solutions with the elementary rod theory

The plate subject to a sinusoidal load shown in Fig. 2 is analyzed using a single element and Fourier and Bessel bases, with 44 and 38 degrees of freedom, respectively.

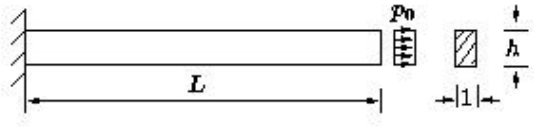

$E = 2 \cdot 10^{11}\,[\mathrm{N/m^2}]$ $\quad p_o = 1\,[\mathrm{N/m}]$

$L = 1\,[\mathrm{m}]$ $\quad w = 700\,[\mathrm{rad/s}]$

$n = 0$ $\quad r = 8 \cdot 10^3\,[\mathrm{kg/m^3}]$

$h = 0{,}1\,[\mathrm{m}]$ $\quad P = p_o h \sin w\,t\,[\mathrm{N}]$

Fig. 2: Plate under sinusoidal axial load

The results presented in Tab. 1 are computed at time t=0.0024 [s] and compared with the analytical solution of the elementary rod theory:

$$u(x,t) = \frac{P \sin kx}{kEA \cos kL} \sin w\,t\,, \qquad \text{where } k = w\sqrt{\frac{r}{E}} \text{ and } P = p_o h\,.$$

	Displacements $\times 10^{-12}$			Axial force $\times 10^{-1}$		
x	Analytic	Fourier	Bessel	Analytic	Fourier	Bessel
0.0	0.00000	0.00000	0.00000	1.00387	1.00387	1.00387
0.2	1.00373	1.00373	1.00373	1.00347	1.00347	1.00347
0.4	2.00668	2.00668	2.00668	1.00229	1.00229	1.00229
0.6	3.00805	3.00805	3.00806	1.00033	1.00033	1.00033
0.8	4.00707	4.00707	4.00707	0.99758	0.99758	0.99758
1.0	5.00294	5.00294	5.00295	0.99404	0.99404	0.99404

Tab. 1: Vibrating rod test.

7.2. Semi-infinite media with known analytical solution

The semi-infinite media with symmetric boundary conditions presented in Fig. 3 has the following analytic solution in displacements,

$$\begin{Bmatrix} u_r \\ u_q \end{Bmatrix} = -2 \begin{Bmatrix} J_1\left(r\frac{|w|}{c_1}\right)\cos w t + Y_1\left(r\frac{|w|}{c_1}\right)\sin w t \\ 0 \end{Bmatrix} \tag{21}$$

where J_1 and Y_1 represent the first order Bessel functions of the first and second kind, respectively. The results obtained for E = 1, ν = 0.25, r =1 and w =1 are presented in Fig. 3.

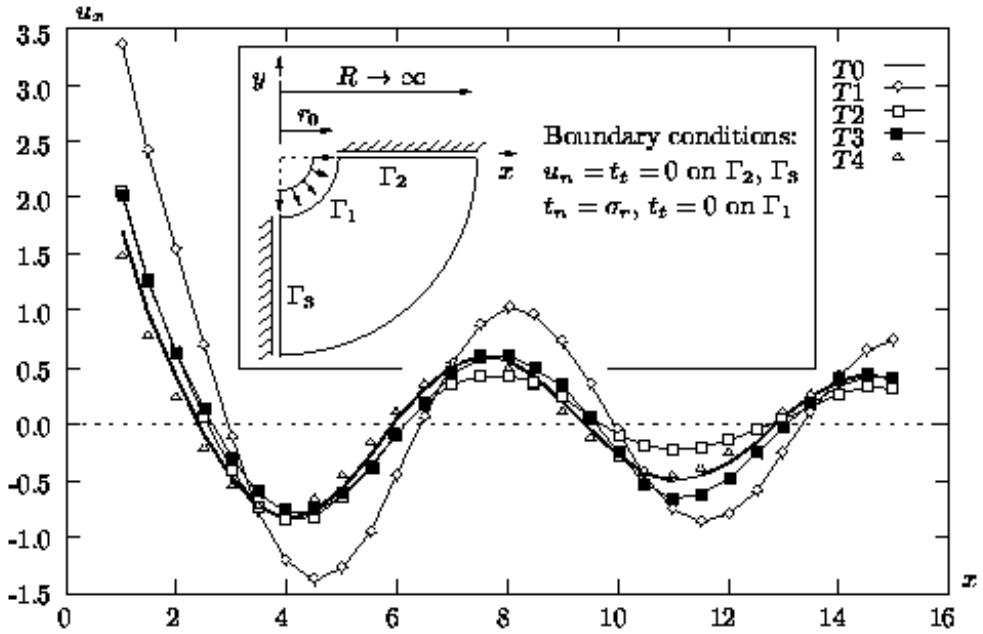

Fig. 3: Horizontal displacement on the side y=0 at t=1.57 s.

When one semi-infinite element is used to solve the problem, test *T*0 in Fig. 3, the exact solution (21) is recovered because it is contained in the Hankel approximation basis.

Tests *T*1 (14 elements with 1644 degrees of freedom) and *T*4 (30 elements with 3484 degrees of freedom) are obtained with bounded elements with absorbing boundary placed at r = 14 and r = 33, respectively. Test *T*2 has 1972 degrees of freedom. It is based on the finite element mesh of test *T*1 with the absorbing boundary being replaced by 4 semi-infinite elements. Test *T*3 is the p-refinement of test *T*2 for 2312 degrees of freedom. Tests *T*1 and *T*4 show that the accuracy of the bounded element solution improves with the distance of the absorbing boundary at the cost of increasing significantly the number of finite elements. The tests with unbounded elements show a faster convergence rate with the advantage of not depending on the choice of positioning the absorbing boundary and at the expense of involving the computation of unbounded integrals.

7.3. Half space subject to an harmonic vertical load

The elastic half space subject to a harmonic distributed load shown in Fig. 4 is investigated in [8, 3]. The dimensionless radiation impedance, defined as

$$\bar{z}_n = -\frac{1}{r\,c_1}\frac{\bar{T}_z}{\dot{\bar{u}}_z} = \frac{1}{r\,c_1}\frac{\bar{T}_z}{w_n}\frac{\mathrm{Im}(\bar{u}_z)+i\,\mathrm{Re}(\bar{u}_z)}{\left|\bar{u}_z\right|^2}$$

where $\bar{u}_z$ is the average vertical displacement under the loading strip, is used to compare the analytical results with the ones obtained using the spectral and the present formulation. The values obtained are given in Tab. 2. where $\bar{w}_n = B w_n / c_1$ is the dimensionless frequency.

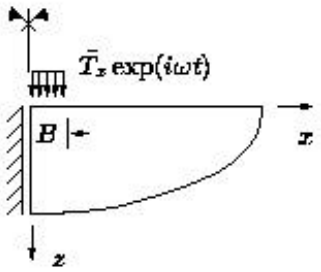

$l = 2.23733 \cdot 10^8\ [\mathrm{N/m^2}]$ $\quad c_2 = 262.674\ [\mathrm{m/s}]$

$m = 1.119 \cdot 10^8\ [\mathrm{N/m^2}]$ $\quad B = 0.5\ [\mathrm{m}]$

$r = 1621.8\ [\mathrm{kg/m^3}]$ $\quad \bar{T}_z = 1\ [\mathrm{N/m^2}]$

$c_1 = 525.308\ [\mathrm{m/s}]$

Fig. 4: Half space subject to a harmonic vertical load.

$\bar{w}_n$	Analytical [8]			Spectral [3]			Hvbrid-Trefftz		
	$\mathrm{Re}(\bar{u}_z)$	$\mathrm{Im}(\bar{u}_z)$	$\lvert\bar{z}_n\rvert$	$\mathrm{Re}(\bar{u}_z)$	$\mathrm{Im}(\bar{u}_z)$	$\lvert\bar{z}_n\rvert$	$\mathrm{Re}(\bar{u}_z)$	$\mathrm{Im}(\bar{u}_z)$	$\lvert\bar{z}_n\rvert$
0.1	1.21	-1.77	2.14	1.29	-1.72	2.15	1.13	-1.79	2.11
0.2	0.96	-0.97	1.36	1.01	-0.94	1.38	0.94	-0.83	1.26
0.3	0.87	-0.66	1.09	0.90	-0.63	1.10	0.70	-0.66	0.96
0.4	0.83	-0.47	0.95	0.86	-0.45	0.96	0. r' 7	-0.20	0.79
0.5	0.81	-0.34	0.88	0.84	-0.32	0.89	0.80	-0.31	0.86

Tab. 2: Dimensionless radiation impedance.

The amplitude of the displacement field is presented in Fig. 5 for the 5 frequencies considered, in domain 0 < r < 35 [m].

Fig. 5: Amplitude of the displacement field ($\overline{w}_1 \ldots \overline{w}_5$).

8. CONCLUSIONS

The use of unbounded elements in the modelling of a semi-infinite media provides a faster convergence of the finite element solution and eliminates the necessity of choosing the position of the absorbing boundary. However these elements involve the numerical computation of highly oscillatory unbounded integrals which represent a hard task from the computational point of view. These numerical difficulties can be avoided using bounded elements; with the cost of having to choose apriori the position of the absorbing boundary. Moreover the convergence of the solution is slower.

9. ACKNOWLEDGMENT

This work is part of the research developed at ICIST, Instituto Superior Técnico, and has been supported by *Fundação para Ciência a Tecnologia* through project PRAXIS/2/2.1/CEG/33/94.

10. REFERENCES

[1] Abramowitz, M. and Stegun, I. (1972), *Handbook of Mathematical Functions With Formulas, Graphs, and Mathematical Tables*, Applied Mathematics Series * 55, National Bureau of Standards, 10th edition.

[2] Achenbach, J. D. (1973), *Wave propagation in elastic solids*, Vo1.16 of *North-Holland Series in Applied Mathematics and Mechanics*, North-Holland Publishing Company, Amsterdam.

[3] Degrande, G. (1992), A *Spectral and Finite Element Method for Wave Propagation* in *Dry and Saturated Poroelastic Media*, Ph.D. thesis, Katholieke Universiteit to Leuven, Belgium.

[4] Freitas, J. A. T. (1997), "Hybrid-Trefftz displacement and stress elements for elastodynamic analysis in the frequency domain", *Computer Assisted Mechanics and Engineering Science*, Vol.4, pp. 345-368.

[5] Freitas, J. A. T. (1998), "Hybrid finite element formulation for elastodynamic analysis in the frequency domain", *International Journal of Solids and Structures*, in press.

[6] Freitas, J. A. T. and C., Cismasiu (1998), "Hybrid-Trefftz Displacement Element for Spectral Analysis of Bounded And Unbounded Media", to be published.

[7] Lysmer, J. and Kuhlemeyer, R. L. (1969), "Finite dynamic model for infinite media", *Journal of the Soil Mechanics and Foundation Division, Proceedings of the ASCE*, Vo1.95, No.SM4, pp. 859-877.

[8] Miller, G. F. and H., P. (1954), "The field and radiation impedance of mechanical radiators on free surface of a semi-infinite isotropic solid", in *Proceedings of the Royal Society of London*, Vol.A 223, pp.521-541.